Adsorption site determination of a large π-conjugated molecule by normal incidence x-ray standing waves: End-capped quaterthiophene on Ag(111)

L. Kilian, W. Weigand, and E. Umbach
Experimentelle Physik II, Universität Würzburg, Am Hubland, D-97074 Würzburg, Germany

A. Langner and M. Sokolowski*
Institut für Physikalische und Theoretische Chemie der Universität Bonn, Wegelerstraße 12, D-53115 Bonn, Germany

H. L. Meyerheim† and H. Maltor
Institut für Kristallographie und Mineralogie der Universität München, Theresienstraße 41, D-80333 München, Germany

B. C. C. Cowie and T. Lee
European Synchrotron Radiation Facility, Boîte Postale 220, F-38043 Grenoble Cedex, France

P. Bäuerle
Abteilung Organische Chemie II, Universität Ulm, Albert-Einstein-Allee 11, D-89081 Ulm, Germany
(Received 1 March 2002; published 19 August 2002)

Using normal incidence x-ray standing waves, we determined the geometric structure of the adsorption site of a large π-conjugated molecule with six rings, end-capped *quaterthiophene* (EC4T), on the Ag(111) surface in the commensurate monolayer. The S 1*s* absorption profiles were measured for the (111) and $(\bar{1}\bar{1}1)$ Bragg reflections. The vertical coherent position $D_{co}^{(111)}$, i.e., the average distance between molecules and Ag surface, was determined to 3.15 ± 0.05 Å. This is less than expected for van der Waals bonding and more than known for a local S-Ag bond, thus revealing that the surface bonding involves the entire conjugated π system, in agreement with earlier photoemission results. The lateral position of the EC4T molecule was obtained from a simulation of the experimental coherent position in $[\bar{1}\bar{1}1]$ direction (1.02 ± 0.1 Å). This results in the first complete determination of the adsorption geometry of a large *flat-lying* organic molecule on an inorganic surface.

DOI: 10.1103/PhysRevB.66.075412 PACS number(s): 68.35.Bs

I. INTRODUCTION

Over the last years a strong interest has evolved in the bonding of large, polycyclic π-conjugated molecules to (inorganic) surfaces and interfaces. This information is important, for instance, for the understanding and optimization of organic film growth,[1,2] electrical contacts to organic films,[3] and interfacial electronic barriers in organic semiconducting devices.[4] Most relevant is of course the precise knowledge of the geometric structure, which includes the internal geometry of the adsorbed molecule and its adsorption site on the surface. On the basis of such data, theoretical calculations could be performed in order to provide more insight into the nature of the chemical bonding of large molecules to surfaces, which is of general interest.

However, the experimental determination of the geometric structure parameters of large organic molecules on surfaces is rather difficult. The determination of the internal geometry, e.g., by surface x-ray diffraction (SXRD),[5,6] is possible but difficult because there are many atoms per unit cell and because these scatter only weakly. The determination of the adsorption site is also difficult, because standard techniques, e.g., LEED (low-energy electron diffraction)-IV analysis, have to cope with unit cells that are considerably larger than those of standard adsorption systems. Other techniques based on surface extended x-ray absorption fine structure (SEXAFS) or photoelectron diffraction suffer from the same problems and require distinct models of the adsorption site, between which they probably cannot decide unambiguously.[7] As a consequence, only very few large molecules have been investigated concerning their adsorption site.

In this paper we report a complete determination of the adsorption site of a large chainlike organic molecule in a *planar* adsorption geometry. This geometry causes that several molecular units and many substrate atoms are involved in the surface bonding. Therefore the situation is rather complex and significantly different compared to that of a large organic molecule bonded to the surface in an upright orientation via one specific functional group, as for instance, in self-assembled monolayers.[8] We used a combination of SXRD and normal incidence standing waves[9,10] (NIXSW) to determine the site of a so-called ''end-capped'' quaterthiophene (EC4T) on Ag(111). The structure formula of EC4T is shown in Fig. 1. EC4T (438 amu) consists of four conjugated thiophene rings and two terminal ''end-caps.'' [11]

From LEED, STM (scanning tunneling microscope) (Ref. 12), SXRD (Ref. 6), and NEXAFS (near-edge x-ray-absorption fine structure) (Ref. 13) investigations, it is known that EC4T adsorbs in a flat geometry with all-trans-conformation of the thiophene rings on the Ag(111) surface. In the monolayer a highly ordered commensurate superstructure with *one* molecule per unit cell is formed (see Fig. 5,

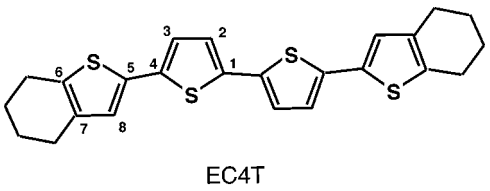

FIG. 1. Structure formula of the end-capped quaterthiophene molecule (EC4T). The labeling of the C atoms is shown for one half of the molecule.

below).[12,14] This implies that all EC4T molecules exhibit the same adsorption site and that there exists a distinct minimum in the lateral corrugation of the surface bonding potential. This is very remarkable for an extended large molecule as EC4T. (For comparison with other end-capped oligothiophenes of chain length 3–6, see Ref. 14).

From *differential* chemical peak shifts in NEXAFS (Ref. 13) and ultraviolet photoemission spectroscopy (UPS) spectra[15] it was concluded that the bonding of the molecule to the surface is *chemisorptive*. Upon annealing of the commensurate EC4T monolayer, no desorption, but dissociation of the EC4T occurs.[12] The comparison of x-ray photoemission spectroscopy (XPS) data (C $1s$ and S $2p$) of the EC4T monolayer and multilayer shows only very small overall shifts of 0.3 eV, as found for physisorbed monothiophene[16] and bithiophene on Ag(111).[17] This reveals that *no* local bonding of the S atoms to the surface via the lone pair occurs, as for instance, found for monothiophene on more reactive substrates.[18] Instead, the entire π system must be involved in the surface bonding. Thus the interesting question, which is the subject of the reported investigation here, arises: What is the specific adsorption geometry and energetically favored adsorption site of this molecule? Especially, we wanted to find out, whether the S atoms in the thiophene rings play a specific role for the surface bonding.

From SXRD (Ref. 6) it was found that the lateral internal molecular bonding distances (i.e., the C═C, C—C, and C—S bonds in the thiophene rings) and the bonding angles of EC4T adsorbed on Ag(111) are significantly modified, i.e., the bonding lengths differ up to about +10% with respect to those of EC4T molecules in a bulk crystal. In a chemical sense, the bonds in the thiophene rings (which are about parallel to the surface) may be weakened by donation of electrons from the substrate into the molecular π system.

The SXRD analysis further reveals that the interatomic vectors between the four S atoms within the molecule are identical for EC4T in a bulk crystal and EC4T adsorbed on Ag(111).[6] This information is most reliable, since the S atoms with a high atomic number lead to the strongest contributions in the Patterson function.[6] The NIXSW experiment reported here measures a signal related to the coherent summation of the positions of these four S atoms relative to the substrate. As we will describe in detail below, the analysis of the NIXSW data requires the knowledge of the interatomic vectors between the four S atoms. Therefore this information from SXRD is an important prerequisite for the adsorption site determination by NIXSW, described in this work.

This paper is organized as follows. Section II contains the experimental details. The data evaluation and computational techniques used for molecular modeling simulations are described in Sec. III. The experimental results are presented in Sec. IV, and a discussion of the observed structure is given in Sec. V. Summarizing conclusions are drawn in Sec. VI.

II. EXPERIMENT

A. General

The experiments were carried out at beam line ID 32 at the European Synchrotron Radiation Facility (ESRF) in Grenoble, France. The beam line is equipped with an UHV surface science end-station consisting of a hemispherical electron analyzer (CHA) ($r=150$ mm), LEED optics, and facilities for sample preparation. The angle between the beam line and the CHA axis was 45°.

B. Sample preparation

The Ag(111) sample was prepared by Ar-ion bombardment and subsequent annealing at 400–500 °C. The surface purity was controlled by XPS. Only a very small contamination of carbon was observed, which is attributed to residual inclusions from the polishing process with diamond paste. The LEED pattern of the Ag(111) surface was brilliant with low background and very sharp spots. EC4T monolayers were prepared by evaporating EC4T onto the surface ($T_s = 300$ K) from a Knudsen cell (0.2–0.5 ML/min).[12] The coverage and the long-range order of the EC4T superstructure were controlled by LEED. Generally we deposited slightly more EC4T than required as ideal coverage for the commensurate monolayer, and then removed the excess coverage by annealing. This leads to brilliant LEED patterns of the commensurate EC4T monolayer, as described in detail in Ref. 12.

C. Data acquisition

Detailed descriptions of the NIXSW technique can be found in Refs. 9 and 10. Very briefly it allows us to determine the position of an adatom relative to a substrate Bragg plane from its relative absorption as a function of the photon energy of the standing wave field (absorption profile). In this work the absorption profiles were obtained by measuring three regions of interest, namely, the Ag MVV Auger line, the S $1s$ XPS line, and the S KLL Auger line (see Fig. 2) as a function of photon energy around the Ag(111) Bragg energy (2627 keV) for normal incidence. The spectra were recorded for the (111) and ($\bar{1}\bar{1}\bar{1}$) Bragg reflections, using a total photon energy range of 6–12 eV (pass energy of the CHA: 93 eV). Typical scan times for one sample preparation were 30–60 min. A typical spectrum for each region of interest is shown in Fig. 2. The Ag MVV and S KLL Auger peaks are composed of several Auger transitions as visible from their fine structure and indicated by the fits. We note that the broad shoulder on the high-binding-energy side (at 2480 eV) of the S $1s$ photoemission peak [Fig. 2(b)] is due to the S LMM Auger line (see below) and not due to chemical decomposition or a different adsorption state of the molecule.

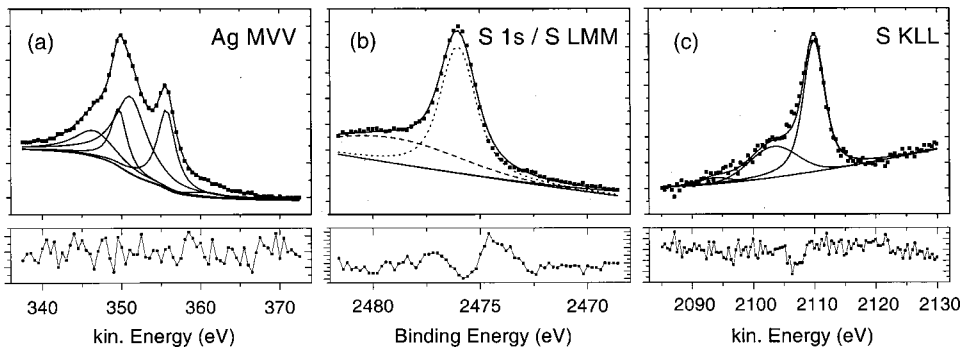

FIG. 2. Typical spectra of the Ag MVV Auger peaks (a), the S 1*s* XPS and S LMM Auger peak (b), and the S KLL Auger peaks (c). These spectra were used to monitor the NIXSW absorption profiles of the substrate and adsorbate, respectively. For all scans, the photon energy was 2.625 eV, i.e., close to the (111) Bragg energy of Ag(111) for normal scattering geometry. The squares mark experimental data, the lines are fitted curves consisting of several peaks, as indicated. Note that the S 1*s* peak (dotted) and S LMM peak (dashed) overlap near the Bragg condition. The bottom panels show the residuum, i.e., $(I_{\mathrm{expt}}-I_{\mathrm{theo}})/I_{\mathrm{expt}}$.

D. Beam damage

Because of the high photon flux we carefully checked for beam-induced damages of the molecular overlayer by measuring the C 1*s* and the S 1*s* XPS spectra prior to and after the NIXSW runs. No changes (e.g., chemical shifts, shoulders, etc.) could be detected, in agreement with previous experiments. In addition, sequentially performed NIXSW runs with reduced resolution and a scan time of 30 min did not show significant changes in the absorption profiles (see below). We thus conclude that beam-induced changes do not play a significant role in this NIXSW experiment. This is also supported by the high values of the measured coherent fractions, which would be much smaller for damaged and structurally disordered layers. Additional checks with LEED after the NIXSW run also proved the stability of the superstructure order, which is sensitive to radiation damage. A slight increase of the diffuse background was likely due to a small decrease of the lateral order or to the adsorption of H_2O from the residual gas.

III. DATA EVALUATION

In a first step, the XPS and Auger spectra were quantitatively evaluated by fitting the spectra by a sum of pseudo-Voigt and Gaussian functions with fixed relative intensities as indicated in Fig. 2. The background was fitted by a polynomial function. The second step consisted of the computing of the absorption profiles, i.e., the relative integrated peak intensities as a function of photon energy. The peak intensities were scaled to the intensity of the incoming photon beam, measured with an I_0 mesh. These absorption profiles (solid symbols) are shown in Fig. 3. Intensity variations due to small movements of the beam position on the sample relative to the electron analyzer have been taken into account by proper correction.

We note that in the energy range around the Ag(111) Bragg energy the kinetic energy of the S 1*s* electrons is very close to the kinetic energy of the S LMM Auger peaks. The Auger structure is the reason for the broad shoulder on the higher-binding-energy side of the S 1*s* peak in Fig. 2(b). As a consequence, the Auger structure shifts across the XPS S 1*s* peak during the scan of the photon energy (see Fig. 4). This overlap of two peaks was taken into account in the data evaluation. For this purpose the positions and shapes of the Auger S LMM and the S 1*s* XPS peaks were determined from a set of overview spectra first (see Fig. 4), and then used to fit the short-range energy spectra (Fig. 2) that were measured for the determination of the absorption profiles. If the S LMM Auger peaks were not properly subtracted, e.g., by using too small a kinetic energy window, artifacts were introduced into the absorption profiles leading to a change in the coherent distance D_{co} by 0.1 Å, whereas the coherent fraction f_{co} was almost uneffected (for D_{co} and f_{co} see below).

In Fig. 3 the solid lines are fits of the theoretical absorption profiles[19] to the experimental data. Each fit yields two main parameters: the coherent position (D_{co}), which is the averaged distance of the atoms of interest with respect to the substrate Bragg plane, and the coherent fraction (f_{co}), which, in brief, is a parameter that describes the displacement of the atoms around D_{co}. These values are summarized in Table I. Besides D_{co} and f_{co}, the fit determined also the mosaic spread of the sample and the width and center of a Gaussian energy profile describing the primary photon beam.

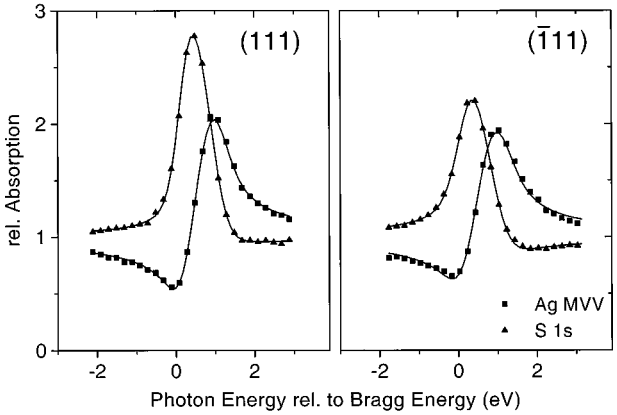

FIG. 3. NIXSW absorption profiles vs. photon energy derived from S 1*s* photoelectrons and Ag MVV Auger electrons in the [111] and $[\bar{1}11]$ directions and best-fitted theoretical curves.

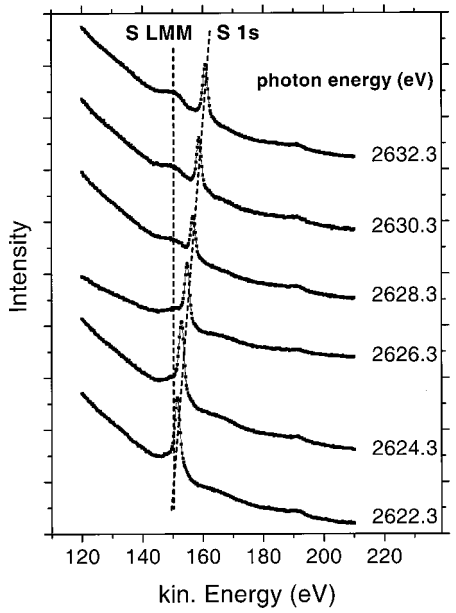

FIG. 4. Overview spectra of the S 1*s* and S LMM region for photon energies around the Bragg energy of 2626 eV. The S 1*s* and S LMM peaks overlap for the photon energies used here. These overview spectra were employed to determine the fitting parameters for line shapes, line positions, and the background.

The x-ray scattering factors were taken from Ref. 20 and calculated using the program ''SHADOW.'' [21]

For high photon energies ($\geqslant$1.5 keV) (Refs. 22 and 23) the role of the nondipolar terms in the photoelectron matrix element has been discussed. We explicitly checked this by a comparison of absorption profiles based on the S 1*s* XPS and the S KLL Auger lines, respectively, in a separate experiment. If nondipolar effects play a role they are expected to cause a difference between the two profiles.[23] However, we found no significant differences, and within a few percent identical values of D_{co} and f_{co} were obtained. This finding is consistent with recent relativistic calculations of nondipolar angular parameters.[24] We thus conclude that nondipolar effects do not play a role for S 1*s* photoelectrons in contrast to, e.g., Ref. 23, where the O 1*s* and O KLL peaks measured for the Ag(111) Bragg plane lead to different absorption profiles. The likely reason is that the spatial extension of the S 1*s* electron wave function is significantly smaller compared to that of the O 1*s* electron.

TABLE I. Summary of the coherent positions and coherent fractions (D_{co} and f_{co}).

Direction	S 1*s*		Ag *MVV*	
	D_{co} (Å)	f_{co}	D_{co} (Å)	f_{co}
[111]	3.15±0.05	0.70±0.05	2.36[a]	0.85±0.05
$[\bar{1}11]$	1.02±0.08	0.48±0.05	2.36[a]	0.78±0.05

[a]These values were fixed to the Ag bulk value during the fit.

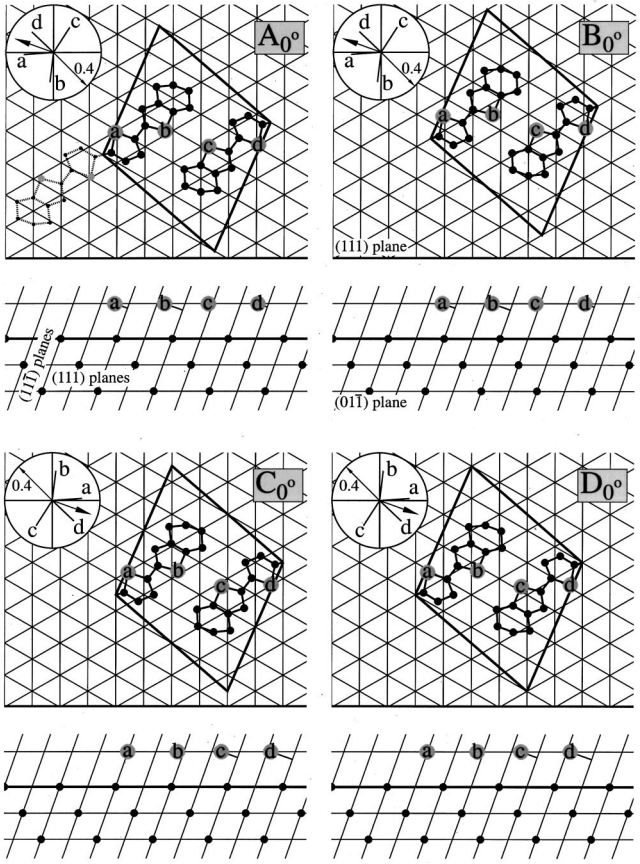

FIG. 5. Comparison of the four symmetry-allowed molecular adsorption sites ($A-D$) of EC4T on Ag(111) and simulation of the position vectors in $[\bar{1}11]$ direction. Only one (out of three possible) rotational domains is displayed, leading to the notation $A_{0°}$, $B_{0°}$, $C_{0°}$, and $D_{0°}$. In the upper part of each panel a top view of the unit cell of EC4T on the Ag(111) substrate lattice is shown. The substrate Ag atoms are at the intersections of the thin lines. The unit cell contains one EC4T molecule that is presented by two half molecules for symmetry reasons. Carbon atoms are in black; sulfur atoms in gray are marked by *a*, *b*, *c*, and *d*. The atomic lateral coordinates of the EC4T molecules are taken from Ref. 6. The lower parts of the figures show a side view, i.e., the projection of the S atom positions onto the $(01\bar{1})$ plane that is perpendicular to both the (111) and the $(\bar{1}11)$ planes. The top view and the side view fit together along the thicker substrate lattice lines. The corresponding $(\bar{1}11)$ position vectors of the considered rotational domains are illustrated in the Argand diagrams in the top left corners of each panel. The four position vectors for the four S atoms are labeled according to the atoms with $a-d$, the arrow represents the resulting sum vector. The radius of the Argand diagrams is always 0.4 as indicated.

IV. RESULTS AND ANALYSIS

Figure 5 schematically shows four possible adsorption sites, with top and side view in each case. Each top view picture displays the adsorbate unit cell of one rotational domain with two halves of the EC4T molecule on the triangular mesh of the Ag(111) surface (a complete molecule is shown in the upper left frame). The various aspects of the evaluation are discussed in the following.

A. Coherent summation

In the following we denote the complex vector representation of the coherent position and coherent fraction (D_{co}, f_{co}) as the *position vector*. This vector is illustrated by an Argand diagram in the complex plane as $f_{co}\exp(2\pi i D_{co}/d)$, where d is the lattice spacing, i.e., $d_{(111)}$ or $d_{(\bar{1}\bar{1}1)}$ (see insets in Fig. 5). Because there are four S atoms, labeled as a, b, c, and d in Fig. 5, per unit cell, the experimentally determined position vectors are vector sums of the position vectors of four individual S atoms.[25] In the [111] direction the three rotational domains of the EC4T superstructure (for details see Ref. 12) yield inequivalent position vectors, albeit the adsorption sites being identical. Thus we have to sum over the three rotational domains, too. However, the position vectors of the two pairwise corresponding reflectional domains are equivalent.

B. [111] direction

From the experimentally determined position vector in the [111] direction we conclude that the average height $d^S_{(111)}$ of the four S atoms is 3.15 ± 0.05 Å with respect to the extended bulk position of the (111) plane of the Ag substrate. Hereby we note that for the clean Ag(111) an IV analysis[26] revealed that the position of the topmost layer coincides with the ideal bulk position, i.e., there is no relaxation of the topmost layer on clean Ag(111). Thus we may expect a negligible relaxation for the EC4T covered Ag(111) too. Furthermore, from the relatively large value of the coherent fraction in the [111] direction (0.70), we deduce that all four S atoms in the unit cell are of the same height, with a deviation of at most ±0.2 Å with respect to the extended (111) Ag bulk planes. The deviation of ±0.2 Å is the upper limit that is consistent with the reduction of the coherent fraction from 0.85 (measured for the substrate) to the value of the coherent fraction of 0.70 (measured for the adsorbate) under the assumption of zero static or thermal disorder in the vertical site distribution of S atoms and the occupation of two distinct vertical positions of the S atoms within the unit cell.

C. $[\bar{1}\bar{1}1]$ direction

From the experimentally obtained position vector in the $[\bar{1}\bar{1}1]$ direction (Table I) we determine the lateral position of the molecule on the surface by comparison with those position vectors that we compute for distinct hypothetical adsorption sites of the molecule. The computation of the latter vectors (named ''simulated'' position vectors in the following) takes into account the internal geometry of the molecule from the SXRD, $d^S_{(111)}$ from above, and the existence of six symmetry equivalent domains (see below). This complicates the analysis and we thus make a few remarks about the simulations before we turn to the final result. In the simulations only perfect structural order is considered. Generally the experimentally determined f_{co} is reduced due to disorder, and hence the measured f_{co} must be smaller than the simulated f_{co}.

1. Symmetry considerations

Among all possible adsorption sites of the molecule we consider *only* those which exhibit a twofold symmetry axis perpendicular to the surface, i.e., those which have $p2$ symmetry. There are several arguments, why we can neglect other sites. First, the unit cell of the pure adsorbate layer containing one molecule [with a conjugated π system with C_{2h} $(p2mm)$ symmetry] has $p2$ symmetry.[12,27] Since the π system is responsible for the chemical bonding to the substrate, it is expected that an adsorption site of $p2$ symmetry is strongly favored. This $p2$ symmetry of the adsorbed EC4T monolayer is also observed in the molecular STM contrast.[12,14] Second, in the SXRD experiment identical intensity variations along the superstructure rods related by a twofold symmetry axis [i.e., (hkl) and $(\bar{h}\bar{k}l)$] were measured.[6] This also indicates a twofold symmetry of the superstructure unit cell and the adsorption site.

A consequence of a twofold symmetry of the adsorption site is that only the topmost Ag layer (with $p6mm$ symmetry) can be relevant for the symmetry, since the semi-infinite Ag(111) surface exhibits no twofold symmetry axis (symmetry group $p3m1$). Therefore, concerning the adsorption of EC4T, the Ag(111) surface exhibits a quasi-sixfold rotational symmetry. On the Ag(111) surface there exist four such possible adsorption sites of the EC4T molecule with twofold symmetry. These ''molecular'' adsorption sites are illustrated in Fig. 5. Three of them (*A*, *B*, and *C*) could be called *bridge sites*, since the center of the molecule is located above the middle between two Ag atoms of the top layer. The site *D* is then an *a-top site*. Due to symmetry reasons, the adsorption site must coincide with the symmetry center of the EC4T molecule.

The lateral coordinates of the EC4T molecule in Fig. 5 are taken from our earlier SXRD measurement.[6] In Fig. 5 we also show the vertical cross sections (side view) along the $(01\bar{1})$ plane, which is perpendicular to the (111) and $(\bar{1}\bar{1}1)$ planes and thus allows us to illustrate the projected distances of the S atoms to both of these planes. The height of the S atoms in the [111] direction is taken from the (111) NIXSW data, described above. In the simulations we assumed the same height for all four S atoms which is consistent with the high coherent fraction value, as discussed above.

For each of the four possible adsorption sites $(A-D)$ there exist three symmetry equivalent rotational domains (rotated by 120° against each other and denoted by the indices 0°, 120°, and 240°) which yield *inequivalent* position vectors for the S atoms with respect to the $(\bar{1}\bar{1}1)$ plane. For example, for the adsorption site *A* these three rotational domains are illustrated in Fig. 6. The other three symmetry equivalent domains, obtained by a reflection of the three domains shown in Fig. 6 lead to the same position vectors in $(\bar{1}\bar{1}1)$ geometry, and thus need not be considered separately, because the corresponding mirror plane is perpendicular to the $(\bar{1}\bar{1}1)$ plane. Thus for obtaining the resulting position vector of *one* adsorption site A, B, C, or D, one has to sum up 12 individual position vectors (four S atoms per unit cell times three rotational domains).

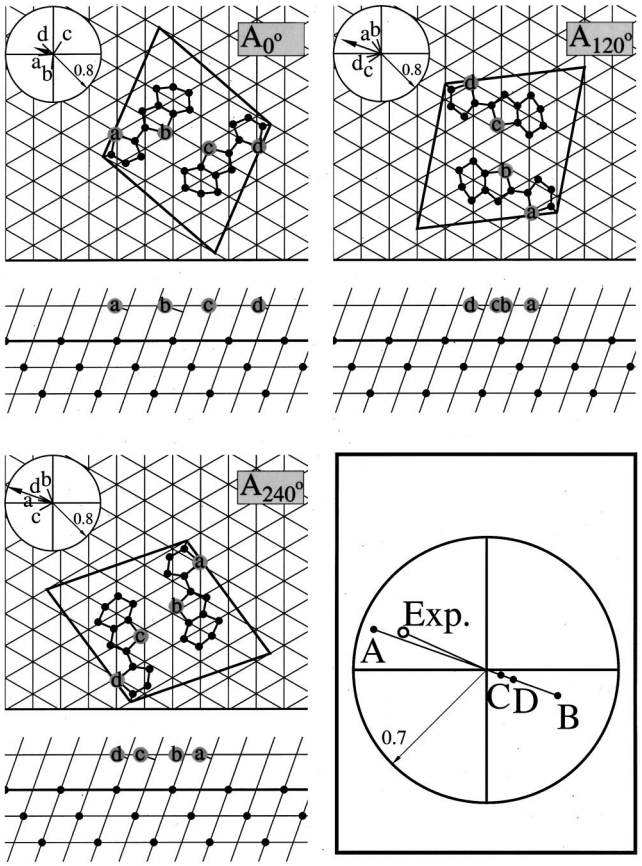

FIG. 6. Comparison of the three rotational domains of the molecular adsorption site *A* of EC4T on Ag(111) and simulation of the $(\bar{1}\bar{1}1)$ position vectors (for details see also figure caption 5). The radius of the Argand diagrams is always 0.8 as indicated. Lower, right panel: Argand diagram of the resulting position vectors in $[\bar{1}\bar{1}1]$ direction of the adsorption sites *A*, *B*, *C*, and *D* after summation of the resulting sum vectors of the three rotational domains. The radius of the Argand diagram is 0.7. The value of the experimentally determined position vector is indicated by an open circle. It is only compatible with site *A*.

2. Resulting position vectors

In Figs. 5 and 6, the inset Argand diagrams illustrate the position vectors of the four S atoms (labeled $a-d$) of the depicted structures and the sum vectors (arrow) of these. The finally resulting position vectors from the superposition of the three rotational domains are labeled *A* to *D* for the four possible adsorption sites and compared with the experimentally determined position vector in the large Argand diagram of Fig. 6 (lower right frame). From this comparison we see that only the position vector of site *A* coincides within experimental error with the experimental position vector. In addition, we can exclude that a relevant fraction of molecules occupies an adsorption site different from *A*, since any admixture of position vectors *B*, *C*, or *D* would yield coherent fractions that are smaller than the experimentally measured, which is not meaningful.

There are several remarkable details in the simulation. First, we note that the pairs of adsorption sites A/B and C/D, respectively, lead to identical position vectors for the rotational domain denoted by 0° in Fig. 5. The reason is that the adsorption site $A_{0°}$ can be transformed into the $B_{0°}$ ($C_{0°}$ into $D_{0°}$, accordingly) by a shift *parallel* to the $(\bar{1}\bar{1}1)$ plane. Furthermore, we observe that the position vectors of $A_{0°}$ and $B_{0°}$ are rotated by 180° [i.e., half a $(\bar{1}\bar{1}1)$ lattice spacing] with respect to those of $C_{0°}$ and $D_{0°}$, since the projections of these sites onto the $(01\bar{1})$ plane can be transformed into each other by a shift of half a lattice constant (see Fig. 5). Similar symmetries also exist between the position vectors of the other rotational domains (not illustrated). In summary, the result of all these is that for all 12 different rotational domains, only *two* different coherent positions are found, which—in addition—differ by half a $(\bar{1}\bar{1}1)$ lattice spacing (represented by two opposite directions in the Argand diagram). This is a consequence of the twofold overall symmetry of the adsorption site that is only compatible with either a zero lateral displacement of the adsorbate relative to the unit cell of the Ag(111) surface (site *D*) or a displacement by half a lattice constant with respect to site *D* ($A-C$).

The coherent fractions (lengths of the arrows) vary significantly within the three rotational domains of one adsorption site (see Fig. 6). However, they depend only on the lateral coordinates of the molecule and the considered rotational domain, and not on the specific adsorption site. As a consequence, the coherent fractions are identical for the structures $A_{0°}$, $B_{0°}$, and $C_{0°}$, and $A_{120°}$, $B_{120°}$, and $C_{120°}$, and so on (see Fig. 5).

It is evident that the resulting simulated position vectors depend on the lateral coordinates of the S atoms in the unit cell, which were taken from the SXRD data. In order to estimate the uncertainty in the position vectors due to the uncertainty in the lateral coordinates, we have deliberately varied the relative lateral coordinates within the unit cell by $\pm 1\%$ (i.e., the error bar of the SXRD analysis[6]) The variations of the resulting position vectors are illustrated in Fig. 7. Figure 7(a) shows the result with a fixed vertical height of 3.15 Å of the S atoms, whereas in Fig. 7(b) an additional deviation from this height by $+0.2$ Å for atoms *a* and *d* and -0.2 Å for atoms *b* and *c* was included. As explained in Sec. IV.B the maximal deviation of ± 0.2 Å can be estimated by the measured value of f_{co}. This type of ''buckling'' leads to two different distinct position vectors in the [111] direction and consequently to a lower coherent fraction in the [111] direction. In both cases the twofold symmetry of the structure was preserved.

In the first case [Fig. 7(a)] we find no dependence of the coherent position on the lateral coordinates (i.e., an error for the direction of the position vector), which is expected and which is due to the twofold symmetry, as noted above in the discussion of the rotational domains. (Strictly speaking, the position vector is of course only fixed modulo half a substrate lattice spacing.) In contrast, the coherent fractions (lengths of the position vectors) are strongly dependent on the lateral coordinates. Nevertheless, the variations of the resulting position vectors for the considered error bar are much too small to allow any other adsorption site than *A* to

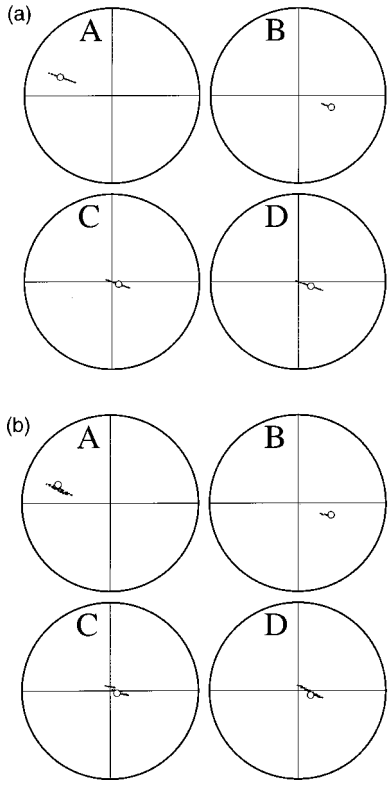

FIG. 7. Analysis of the influence of small variations of the intramolecular lateral coordinates on the simulated $(\bar{1}11)$ position vectors with constant height of the S atoms (a) and including small height deviations of ± 0.2 Å (b). The open circles resemble the simulated position vectors of the four considered adsorption sites $A-D$ using the best value of the lateral coordinates determined by SXRD (Ref. 6). The lines (a) and black areas (b) consist of individual points which represent position vectors for lateral coordinates that deviate by 1% from the best value determined by SXRD (Ref. 6). The two-fold symmetry was preserved. Only the coherent fractions corresponding to the lengths of the position vectors show a considerable dependence on the lateral coordinates. The radius of the Argand diagrams is always 0.7. For further details see text.

fit the experimental data [see Fig. 7(a)].

The situation is slightly different in the second case [Fig. 7(b)]. Here variations of $D_{\mathrm{co}}^{(\bar{1}11)}$ result from the additional vertical displacement. The maximal possible variation of $D_{\mathrm{co}}^{(\bar{1}11)}$ can be estimated as $(\pm 0.2\ \text{Å})[\cos(70.5°)] = \pm 0.067\ \text{Å} = \pm 3\% d(\bar{1}11)$. However, the actual variation depends on the specific lateral coordinates of the S atoms. Again we find for this deviation from our start values that the conclusion of adsorption site *A* is not effected. Nevertheless, the observed strong dependence of the coherent fraction on the lateral internal molecular coordinates indicates that a meaningful analysis requires the knowledge of these with high precision with respect to the length scale of the considerably smaller *substrate* unit cell. To fulfill this criterion may be increasingly difficult with increasing size of the organic molecules under investigation. In the present work we are in a safe situation, since the interatomic vectors between the S atoms (and thus the lateral coordinates) are known from SXRD with high precision, and were found to agree with those of the molecule in the bulk.

V. DISCUSSION

From the experimental results we derived that in the commensurate monolayer structure of EC4T on Ag(111) the adsorption site labeled *A* in Fig. 5 is occupied with very high preference. The two S atoms of the two inner thiophene rings (*a* and *d*) are located nearly exactly on *a*-top sites (within error of the analysis) and those of the two outer thiophene rings (*b* and *c*) are also very close to *a*-top sites. The distance to the nearest-neighbor Ag atoms ($d_{\mathrm{S\text{-}Ag}}$) is calculated from $D_{\mathrm{co}}^{(111)}$ as 3.16 Å for the S atoms *a* and *d* and as 3.26 Å for the S atoms *b* and *c*, respectively. Such large $d_{\mathrm{S\text{-}Ag}}$ values and an adsorption close to the *a*-top site are in gross contrast to the general trend for chemisorbed *atomic* S to adsorb in high-symmetry sites on close-packed metal surfaces.[28] This site would be a threefold S site (fcc or hcp) here, which would lead to $d_{\mathrm{S\text{-}Ag}}$ values around 2.3 Å.[28] The sites of the S atoms observed here are also remarkably different from the site of S observed for alkylthiols adsorbed on Ag(111), which was identified as a threefold hollow site from SEXAFS measurements.[8] An *a*-top site of the S was observed for monothiophene adsorbed on Cu(111) in a flat-lying geometry,[29] however, the value of $d_{\mathrm{S\text{-}Cu}} = 2.60$ Å was considerably smaller there. The here observed S-Ag bond distances are also remarkably larger than those on bulk compounds such as Ag_2S,[30] i.e., 2.49–2.69 Å or those values observed for thiophene-Ag complexes in solution which are around 2.9 Å.[31]

Therefore we can exclude strongly localized bonds between the S atoms and the Ag surface. Moreover, we must conclude that the distinct adsorption geometry with its relatively large vertical distance and the chemisorptive, covalent nature of the EC4T/Ag(111) surface bonding is not related to a covalent bonding of the S atoms to the surface. Instead it has to be explained by a surface bonding involving the entire π system of the molecule (involving S and C atomic orbitals) as also deduced from electron spectroscopic data and the distortion of the internal bonds observed in SXRD (see above). This finding is corroborated by the above-mentioned absence of XPS core level shift differences between the C and S atoms when EC4T multilayer and monolayer molecules are compared.[15,16]

The Ag-S bond distance is, however, smaller than the sum of the Ag and S van der Waals radii, which is 3.5 Å [1.7 + 1.8 Å (Ref. 32)] and is also still slightly smaller (at least for the atoms *a* and *d*) than the sum of the atomic radius of Ag metal (1.45 Å) plus the S van der Waals radius, i.e., 3.25 Å.[32] This finding indicates that the EC4T molecules are *not* physisorbed on the Ag(111) surface, but that at least weak chemisorption occurs, in agreement with the above-mentioned results from various electron spectroscopies.

We further consider the C atoms in the thiophene rings which we cannot directly observe by our experiment. In the simplest adsorption geometry, all four thiophene rings would be fully planar to the surface. This geometry is supported by the strict dichroism observed in NEXAFS experiments.[13] It

would imply that all four thiophene rings, i.e., the entire aromatic part of the molecule, are 3.15 Å above the Ag(111) plane with a maximal deviation of ±0.2 Å (see above). It is interesting to compare this bond distance with values found for other aromatic adsorbates. For instance, for benzene on close-packed metal surfaces a much smaller bond distance of about 2.5–2.6 Å [e.g., on Ru(0001) (Ref. 33)] is observed, whereas for the large aromatic and planar molecule PTCDA (perylene-3,4,9,10-tetracarboxylic-3,4,9,10-dianhydride) on Ag(111) an only slightly smaller vertical bond distance of 2.9 Å is found.[34] This difference to PTCDA can be understood by the different π systems of EC4T and PTCDA and may be partially related to the role of the empty *d* orbitals of the S atoms in the covalent bonding of EC4T to Ag(111) (whereas O atoms are involved in PTCDA). There are indications that the bonding of EC4T to Ag(111) is significantly weaker compared to PTCDA/Ag(111), because chemical shifts in UPS spectra of EC4T/Ag(111) are smaller compared to those observed for PTCDA/Ag(111) and because at higher coverage an incommensurate monolayer structure with non-site-specific adsorption exists for EC4T, but not for PTCDA.[2,12] Thus a very interesting aspect of our experimental results is that for the commensurate phase of EC4T/Ag(111) we find a bond distance for a site-specific adsorption which is rather large.

However, since our experiment measures solely the positions of the S atoms, we can of course not exclude the fact that the thiophene rings are not fully planar to the surface, but are slightly inclined by a few degrees such that the C atoms opposite to the S atoms are closer to the surface than the S atoms. Because of the trans configuration of the molecule this would cause an alternating inclination of the rings along the molecular axis. A small inclination of a few degrees would be still compatible with the dichroism observed in NEXAFS, and is also fully compatible with the SXRD results, since the SXRD measurements did not provide an out-of-plane resolution high enough to yield information on subtle ''vertical disorder.'' Small ring tilts of 5° to 10° would yield bonding distances of the C atoms (i.e., atoms 2, 3, 7, and 8, see Fig. 1) to the top Ag(111) plane of 2.7–2.9 Å. Such a ring inclination is especially possible for the two inner thiophene rings, whereas it may be more hindered for the outer rings due to the endcaps (see Fig. 5). Such tilts should be especially relevant for the interpretation of the STM tunneling contrast observed for EC4T (Ref. 12) and would be also an interesting aspect of theoretical calculations of this site geometry.

Finally, we discuss the lateral position of the molecule on the surface. In the final structure model in Fig. 8 there are three interesting features that may be relevant for the final lateral position of the molecule: First, as already noted, the S atoms are close to *a*-top sites. Second, the four C-C bonds of the atoms 2–3, and 7–8 (see Fig. 1 for notation) in the four thiophene rings are about parallel to the direction of close-packed Ag atoms ([001] direction). And third, the centers of the two terminal endcaps appear to be exactly on *a*-top sites. At this point we can, of course, only speculate about which of these features is relevant for the lateral position or whether even a combination of them is important. This can only be derived from adequate cluster or slab calculations.

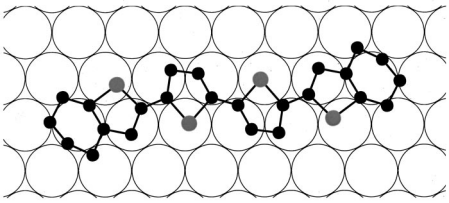

FIG. 8. Hardsphere model of EC4T on the Ag(111) surface illustrating the finally determined adsorption site *A*. For further details see text.

Since the endcaps hardly belong to the aromatic system of the molecule, we assume that their position is less relevant; it possibly supports the site selectivity by additional weak physisorptive bonds of the endcaps to the surface. As discussed above, due to the large bond distance of the S atoms and due to the XPS data a site-selective local bond of the S atoms can be ruled out. Therefore, we arrive at the conclusion that the interaction of the π system of the thiophene rings with the substrate determines the lateral position. The bonding thus involves the four C atoms and one S atom per thiophene ring and probably the three Ag atoms close to each thiophene ring, as illustrated in Fig. 8. Thus we conclude a bonding mechanism of the molecule to the surface, which is spatially rather extended, but—possibly through a cooperative effect of the bonding forces on the four rings—causes a distinct minimum of the resulting lateral corrugation of the molecule-to-surface bonding potential leading to the preference of a specific adsorption site. A hint for the relevance of such a cooperative effect may be that the identified adsorption site *A* exhibits the highest coherent fraction (in the $[\bar{1}11]$ direction) of the four considered sites. A high coherent fraction indicates that the lateral distances of all S atoms (and conclusively also of the thiophene rings) with respect to the underlying Ag(111) lattice are similar.

VI. SUMMARY AND CONCLUSIONS

Using the NIXSW technique we have determined the exact adsorption site of a large aromatic oligomer (EC4T) chemisorbed on the Ag(111) surface in a planar geometry. Our analysis is based on the NIXSW absorption profiles in $[111]$ and $[\bar{1}11]$ direction of the four S atoms in the four thiophene rings of the molecule and involves the internal bond distances known from SXRD. We can clearly discriminate the correct adsorption site from other adsorption sites, which are also compatible with the symmetry of the adsorption system. One prerequisite for this analysis is the high coherent fraction of the correct site in $[\bar{1}11]$ direction. This high coherent fraction is remarkable, since due to incoherent superposition of the four S atoms per molecule and three rotational domains, one may have expected a very small coherent fraction. We speculate that a high coherent fraction is a characteristic feature for the situation where extended periodic molecules exhibit a well-defined adsorption site.

The four S atoms per EC4T molecule are located (3.15 ±0.2) Å above the topmost Ag(111) plane and come close

to *a*-top positions. The rather long S-Ag bond distance indicates a delocalized bonding of the molecule and excludes a strong local S-Ag bonding. From the significantly smaller distance, as compared to van der Waals radii, as well as from photoemission data we conclude that a covalent bonding of the entire molecule to the substrate occurs. However, small tilts of the thiophene rings by a few degrees which bring the C atoms closer than 3.15 Å to the Ag surface cannot be excluded from our data and may be relevant for the understanding of the bonding mechanism. Such tilts are also plausible because of the strong internal distortions observed in SXRD.

ACKNOWLEDGMENTS

We thank Dr. D. Gudat, Dr. G. Held, Dr. F. Schreiber, and M. Voigt for helpful discussions. We are grateful for the financial and experimental support of this work by the ESRF, Grenoble. This project was further financially supported by the Deutsche Forschungsgemeinschaft under the Grant No. So407/2. One of us (E.U.) would like to thank the Fond der Chemischen Industrie for financial support.

*Corresponding author. FAX: +49 (0)228-73 2551. Email address: sokolowski@thch.uni-bonn.de

†Permanent address: Max-Planck-Institut für Mikrostrukturphysik, Weinberg 2, D-06120 Halle, Germany.

[1] N. Karl and Ch. Günther, Cryst. Res. Technol. **34**, 243 (1999).

[2] E. Umbach, M. Sokolowski, and R. Fink, Appl. Phys. A: Mater. Sci. Process. **63**, 565 (1996).

[3] S. Forrest, Chem. Rev. **97**, 1793 (1997).

[4] H. Ishii, K. Sugiyama, E. Ito, and K. Seki, Adv. Mater. **99**, 605 (1999).

[5] H. L. Meyerheim, Th. Gloege, M. Sokolowski, E. Umbach, and P. Bäuerle, Surf. Rev. Lett. **6**, 883 (2000).

[6] H. L. Meyerheim, Th. Gloege, M. Sokolowski, E. Umbach, and P. Bäuerle, Europhys. Lett. **52**, 144 (2000).

[7] C. S. Fadley, Surf. Sci. Rep. **19**, 231 (1993).

[8] D. A. Hutt, E. Cooper, and G. J. Leggett, Surf. Sci. **397**, 154 (1998).

[9] J. Zegenhagen, Surf. Sci. Rep. **18**, 1999 (1993).

[10] D. P. Woodruff, Prog. Surf. Sci. **57**, 1 (1998).

[11] P. Bäuerle, Adv. Mater. **4**, 102 (1992).

[12] C. Seidel, A. Soukopp, R. Li, P. Bäuerle, and E. Umbach, Surf. Sci. **374**, 17 (1997).

[13] M. Bäßler, PhD thesis, University of Würzburg, 1997.

[14] A. Soukopp, K. Glöckler, P. Kraft, S. Schmitt, M. Sokolowski, E. Umbach, E. Mena-Osteritz, P. Bäuerle, and E. Hädicke, Phys. Rev. B **58**, 13 882 (1998).

[15] A. Soukopp, PhD thesis, University of Würzburg, 1997.

[16] K. M. Baumgärtner, M. Volmer-Uebing, J. Taborski, P. Bäuerle, and E. Umbach, Ber. Bunsenges. Phys. Chem. **95/11**, 1488 (1991).

[17] P. Väterlein, M. Schmelzer, J. Taborski, T. Krause, F. Viczian, M. Bäßler, R. Fink, E. Umbach, and W. Wurth, Surf. Sci. **452**, 20 (2000).

[18] B. Sexton, Surf. Sci. **163**, 99 (1985).

[19] Program code used to compute the absorption profiles, private communication by B. C. C. Cowie.

[20] National Institute of Standards and Technology (NIST), physical reference data http://physics.nist.gov/PhysRefData/.

[21] X-ray ray tracing program ''SHADOW,'' private communication by B. C. C. Cowie.

[22] C. J. Fisher, R. Ithin, R. G. Jones, G. J. Jackson, D. P. Woodruff, and B. C. C. Cowie, J. Phys.: Condens. Matter **10**, L623 (1998).

[23] F. Schreiber, K. A. Ritley, I. A. Vartanyants, H. Dosch, J. Zegenhagen, and B. C. C. Cowie, Surf. Sci. **486**, L519 (2001).

[24] V. I. Nefedov, V. G. Yarzhemsky, I. S. Nefedova, M. B. Trzhaskovskaya, and I. M. Band, J. Electron Spectrosc. Relat. Phenom. **107**, 123 (2000).

[25] D. P. Woodruff, B. C. C. Cowie, and A. R. H. F. Ettema, J. Phys.: Condens. Matter **6**, 10 633 (1994).

[26] E. A. Soares, V. B. Nascimento, V. E. de Carvalho, C. M. C. de Castilho, A. V. de Carvalho, R. Toomes, and D. P. Woodruff, Surf. Sci. **419**, 89 (1999).

[27] For a detailed discussion of the symmetry of the EC4T molecule, see Ref. 14.

[28] D. Jürgens, G. Held, and H. Pfnür, Surf. Sci. **303**, 77 (1994).

[29] P. Milligan, J. M. Namarra, B. Murphy, B. C. Cowie, D. Lennon, and M. Kadodwala, Surf. Sci. **412/413**, 166 (1998).

[30] R. W. G. Wyckoff, *Crystal Structures* (Wiley, New York, 1963), Vol. 1.

[31] G. C. van Stein, G. van Koten, F. Blank, L. C. Taylor, K. Vrieze, A. L. Spek, A. J. M. Duisenberg, A. M. M. Schreurs, B. Koji-Prodić, and C. Brevard, Inorg. Chim. Acta **98**, 107 (1985).

[32] N. Wiberg, *Holleman—Wiberg, Lehrbuch der Anorganischen Chemie* (Walter de Gruyter, Berlin, 1995).

[33] W. Braun, G. Held, H.-P. Steinrück, C. Stellwag, and D. Menzel, Surf. Sci. **475**, 18 (2001).

[34] F. Schreiber, S. Sellner, A. Dürr, K. Ritley, H. Dosch, B. C. C. Cowie, and J. Zegenhagen, Verhandl. Deutsche Phys. Ges. (VI) **36**, 500 (2001).